

RESEARCH ARTICLE

Ontogenetic change in predicted acoustic pressure sensitivity in larval red drum (*Sciaenops ocellatus*)

Andria K. Salas^{1,*‡}, Preston S. Wilson² and Lee A. Fuiman³

ABSTRACT

Detecting acoustic pressure can improve a fish's survival and fitness through increased sensitivity to environmental sounds. Pressure detection results from interactions between the swim bladder and otoliths. In larval fishes, those interactions change rapidly as growth and development alter bladder dimensions and otolith–bladder distance. We used computed tomography imagery of lab-reared larval red drum (*Sciaenops ocellatus*) in a finite-element model to assess ontogenetic changes in acoustic pressure sensitivity in response to a plane wave at frequencies within the frequency range of hearing by fishes. We compared the acceleration at points on the sagitta, asteriscus and lapillus when the bladder was air filled with results from models using a water-filled bladder. For larvae of 8.5–18 mm in standard length, the air-filled bladder amplified simulated otolith motion by a factor of 54–3485 times that of a water-filled bladder at 100 Hz. Otolith–bladder distance increased with standard length, which decreased modeled amplification. The concomitant rapid increase in bladder volume partially compensated for the effect of increasing otolith–bladder distance. Calculated resonant frequency of the bladders was between 8750 and 4250 Hz, and resonant frequency decreased with increasing bladder volume. There was a relatively flat frequency dependence of these effects in the audible frequency range, but we found a small increase in amplification with increasing excitation frequency. Using idealized geometry, we found that the larval vertebrae and ribs have negligible influence on bladder motion. Our results help clarify the auditory consequences of ontogenetic changes in bladder morphology and otolith–bladder relationships during larval stages.

KEY WORDS: Fish, Larvae, Ontogeny, Hearing, Otoliths, Modeling, Computed tomography

INTRODUCTION

Larval fishes use a suite of sensory cues to perceive and respond to their environment. Sound is but one of these, yet the physics of this sensory modality (long-distance propagation and relative independence from water movements) make it a valuable source of information in the underwater environment (Montgomery et al., 2006; Atema et al., 2015). Sound can guide larval fishes to benthic habitat (Tolimieri et al., 2000; Simpson et al., 2005, 2010), indicate


habitat suitability for settlement (Parmentier et al., 2015; Gordon et al., 2018) and warn of the threat of predators (Fuiman, 1989; Blaxter and Fuiman, 1990). Vocalizations produced by larval fish may help maintain group cohesion (Staaterman et al., 2014). Using sound as a source of information can improve survival, and traits that enhance sound detection are likely to be under selection (Braun and Grande, 2008) during the larval period. Qualities that improve audition include an ability to detect sounds at lower amplitudes and across a broader range of frequencies, and an ability to discern the direction of a sound's source. These auditory capabilities either require or are improved by the pressure component of sound (Myrberg and Fuiman, 2006; Braun and Grande, 2008). Pressure detection is made possible by the presence of an air bubble that is either mechanically coupled or in close proximity to the otoliths (Popper and Fay, 2011). Otoliths are six calcareous masses in the head, organized into three pairs, that mediate sound detection. Each otolith is closely associated with a sensory macula which contains hair cells that trigger nerve impulses by neurotransmitter release when they are mechanically deflected by motion of the macula relative to the otolith. An inflated swim bladder can allow for an interaction between the otoliths and bladder, enabling the detection of the pressure component of sound in certain species (Popper and Fay, 2011). Thus, larval fishes with an inflated bladder may detect pressure (Myrberg and Fuiman, 2006), potentially refining survival behaviors, such as settlement, that are elicited by auditory cues.

All fishes can detect sound through the particle motion component of a longitudinal acoustic wave, known as direct stimulation (Popper and Lu, 2000). Water particles undergo compression and rarefaction in response to an acoustic stimulus; a fish's tissues, composed mainly of water, move in sympathy. Motion of the denser calcareous otoliths lags that of the surrounding tissue and this differential motion deflects the hair cells of the maculae. In addition to the particle motion external to the fish, there can be a secondary source of particle motion that is produced inside the fish which can contribute to hearing, known as indirect stimulation (Popper and Lu, 2000). The swim bladder pulsates in response to the pressure changes associated with the acoustic wave, thereby re-radiating the energy. This energy aids sound detection if there is a mechanical coupling (e.g. Weberian ossicles) between the swim bladder and otoliths, or if the distance between the bladder and inner ear is small enough to allow the particle motion created by the bladder to reach the otoliths (Popper and Fay, 2011). Anterior swim bladder extensions in adult fishes can position the bladder to within 1 mm of the otoliths, and fishes with this adaptation have more sensitive hearing compared with that of fishes without these bladder extensions (Braun and Grande, 2008; Parmentier et al., 2011; Schultz-Mirbach et al., 2012). The small body size of fish larvae can also position the swim bladder and otoliths very close to one another (e.g. within 1 mm; Atema et al., 2015; Webb et al., 2012), potentially allowing pressure sensitivity. With ontogeny, however, the distance between the otoliths and bladder increases, possibly

¹The University of Texas at Austin, Integrative Biology Department, Austin, TX 78712, USA. ²The University of Texas at Austin, Mechanical Engineering Department, Austin, TX 78712, USA. ³The University of Texas at Austin, Marine Science Institute, Port Aransas, TX 78373, USA.

*Present address: Woods Hole Oceanographic Institution, Biology Department, Woods Hole, MA 02543, USA.

‡Author for correspondence (aks2515@gmail.com)

 A.K.S., 0000-0003-0542-1448; L.A.F., 0000-0003-2667-2684

reducing or eliminating pressure sensitivity unless bladder extensions develop.

Ontogenetic change in auditory thresholds is not consistent across the species tested, with observations of increasing, decreasing and no significant ontogenetic change in hearing sensitivity (e.g. Kenyon, 1996; Wright et al., 2011; Webb et al., 2012). Many factors contribute to the reception and perception of acoustic stimuli (e.g. hair cell number, density and nerve innervation patterns; Webb et al., 2012), and how these factors develop relative to one another will dynamically influence the cumulative auditory response. Morphological factors that change with larval development and impact the likelihood of pressure detection and its sensitivity include characteristics of the swim bladder (e.g. size, shape and material properties of the bladder wall) and the distance between the bladder and inner ear (Popper and Fay, 2011; Webb et al., 2012). As these features develop, a concomitant ontogenetic change in whether and how pressure contributes to audition is expected, thereby shifting the relative contributions of indirect and direct stimulation to audition. Pressure detection through indirect stimulation increases the distance from sound sources at which acoustic cues and signals are detectable (compared with estimates for larvae using particle motion alone), with potential effects on survival and success. For example, a greater detection distance of the acoustic cues used by larvae during settlement increases navigational success (Staaterman et al., 2012) and would provide information sooner about habitat suitability (Parmentier et al., 2015; Gordon et al., 2018). Thus, there can be ecological consequences to a larva's sensitivity to pressure and how this sensitivity changes ontogenetically. We may therefore underestimate the consequences of changing soundscapes for larval settlement and survival if we assume that particle motion is the only relevant acoustic stimulus (as in Mann et al., 2007; Kaplan and Mooney, 2016; Nedelec et al., 2016). The small sizes of larval body plans warrant consideration that they are pressure sensitive. In this study, we used a combination of micro-computed tomography (microCT) and finite-element modeling (FEM) to explore the hypothesis that there is an ontogenetic decrease in the magnitude of indirect stimulation received at the otoliths due to an increase in otolith-to-bladder distance with development, and this reduces a larva's sensitivity to sound pressure. The amount of energy received at the otoliths from the bladder is partially influenced by the bladder's frequency response, so we also modeled the amplitude of the bladder's motion in its response to a range of biologically relevant frequencies. Lastly, we predicted the influence of the larval vertebrae and ribs, which press into the bladder, on the predicted indirect stimulation at the otoliths.

MATERIALS AND METHODS

Study species and rearing of *Sciaenops ocellatus* larvae

We conducted experiments on the temperate and subtropical species *Sciaenops ocellatus* (Linnaeus 1766), known as the red drum. *Sciaenops ocellatus* is a member of the Family Sciaenidae, which is known for sound production (Ramcharitar et al., 2006a; Parmentier et al., 2014). Males produce advertisement calls to court females, and adults have swim bladders with anterior extensions, which are not present in larval stages. Spawning occurs offshore and larvae likely employ multiple sensory systems to locate the preferred settlement habitat of seagrass (Montgomery et al., 2006; Havel, 2014; Havel and Fuiman, 2016). Sound is expected to be a sensory modality used by these fish (Havel, 2014), which have highest auditory sensitivity to low-frequency sounds (100–300 Hz; Horodysky et al., 2008; Havel, 2014), a trend observed for many species (Wright et al., 2005, 2010, 2011).

All work was compliant under the University of Texas at Austin Animal Care and Use approval (AUP-2016-00011). Eggs were obtained from broodstock that were maintained in 12,000–16,000 l re-circulating tanks at the Fisheries and Mariculture Laboratory of the University of Texas Marine Science Institute in Port Aransas, TX, USA, and the Coastal Conservation Association Marine Development Center of Texas Parks and Wildlife Department in Corpus Christi, TX, USA. Broodstock were induced to spawn using temperature and photoperiod manipulation. Eggs were collected in the morning, and for each batch of eggs, 5–10 ml of eggs (ca. 5000–10,000 eggs) was placed into a 150 l cone-shaped tank equipped with internal biofilters and gently aerated. Temperature, salinity and dissolved oxygen were maintained at $27.5 \pm 0.5^\circ\text{C}$, 31 ± 1 ppt and $>7.0 \text{ mg l}^{-1}$, respectively, and monitored throughout the rearing period and adjusted as needed. Photoperiod was maintained at 12 h light:12 h dark.

On days 3–11 post-hatching, larvae were fed enriched rotifers (*Brachionus plicatilis*, L-strain) twice daily at a concentration of 5 rotifers per ml, and on days 10 and 11 post-hatching, all larvae were additionally fed newly hatched *Artemia* sp. nauplii. From 12 days post-hatching onward, larvae were fed *Artemia* sp. twice daily at a concentration of 250–400 l^{-1} . Rotifers were enriched with Algamac 3050 (0.2 g of enrichment per one million rotifers; Aqua-fauna Bio-Marine; www.aquafauna.com) for 45–60 min prior to feeding. *Artemia* sp. were enriched overnight with Algamac 3050 (0.3 g of enrichment per 100,000 *Artemia* sp.). Upon reaching 21 days post-hatching (9–10 mm total length), fish were co-fed a 250 μm microdiet (52% crude protein, Otohime; Reed Mariculture, Campbell, CA, USA) and enriched *Artemia* sp.

Fish were collected at random on days 21–27 post-hatching, depending on target size. We used standard length (SL) to select larvae for inclusion in the study. We used larvae that ranged from 8.5 to 18 mm SL, which represents fish at pre-settlement, settlement and post-settlement stages (Havel et al., 2015). Larval fish were euthanized using an overdose of tricaine methanesulfonate (MS 222), placed individually into Eppendorf tubes, and transported in a cooler with ice to the University of Texas High-Resolution X-ray CT Facility in Austin, TX, USA, for scanning the same day.

CT scanning of *S. ocellatus* larvae

Swim bladder and otolith features were measured using microCT imagery. The high-resolution X-ray CT (HRXCT) data were acquired on a Zeiss (formerly Xradia) MicroXCT 400. The X-ray source was set to 70 kV and 10 W and no X-ray prefilter was employed. The source–object distance was 37 mm and the detector–object distance was 12 mm. Using the 4 \times objective, 721 views were acquired over 360 deg of rotation, with 2 s per view. The resulting HRXCT volumes comprised 851–1508 slices with a voxel size of 5.08, 5.42 or 5.72 μm . Resolution was determined by fish size, as larger specimens required a lower magnification to fit the features of interest within the scan volume.

We imported the stack of images into the image processing software ImageJ (v.1.52g) and converted the files from 16 bit to 8 bit. These files were imported into Avizo software (v.9.5.0), where the bladders and otoliths were segmented using the 3D magic wand tool and then smoothed. The segmented volumes were calculated in Avizo and their surface models exported as stereolithography (STL) files for use in the FEM mesh.

FEM of the acoustic response of the swim bladder

We used the images of the swim bladder and otoliths in FEM (*sensu* Schilt et al., 2012; Cranford et al., 2010; Cranford and Krysl, 2015)

to predict the relative contributions of indirect and direct stimulation at the otoliths in larvae at different developmental stages. We imported the STL files obtained from microCT imagery into MeshLab (v.2016) and down-sampled using a quadratic edge collapse decimation at 50% reduction, applied twice or thrice, depending on bladder size. This was done to reduce superfluous spatial resolution, which in turn reduced the FEM size and improved the speed of the FEM solution without altering the results. We created two STL files for each fish: one of the swim bladder alone and a second that included the six otoliths. We imported these STL files into the FEM software COMSOL Multiphysics (v.5.2a) to simulate the responses of these structures to an acoustic plane wave at frequencies relevant to fish hearing. The model domain consisted of a fluid sphere, and was assigned the model default acoustic properties of water (sound speed 1481 m s^{-1} , density 1000 kg m^{-3}). The approximate center of the bladder was located in the center of the sphere. This water sphere represented both the body of the fish (assuming fish tissues have approximately the same properties as water; Tavolga, 1971) and the environment surrounding the fish. The water sphere had a diameter of 200 mm, which is approximately 50 times larger than the longest swim bladder in our sample. The swim bladder was assigned the model default acoustic properties of air (sound speed 343 m s^{-1} , density 1.204 kg m^{-3}), and functioned as a bladder-shaped air bubble in the model.

In COMSOL, we used a Pressure Acoustics-Frequency Domain module coupled with Solid Mechanics and an Acoustic-Structure Boundary. We applied a spherical radiation condition at the boundary of the domain, with the source of the scattered field located in the center of the swim bladder. The excitation was an incident plane wave consisting of a sinusoid of various frequencies that approached the fish laterally, with a pressure amplitude of 1 Pa for all simulations. The water sphere, swim bladder and otoliths were assigned a finite-element mesh, which divided the model into sub-domains called elements, over which the set of equations were solved. A criterion of quadratic elements sized no larger than 0.2λ was enforced to control both discretization and pollution errors (Ihlenburg, 1998).

We tested whether the size of the water sphere was appropriate to model the system of interest by comparing the analytical and FEM solutions for the resonant frequency of a spherical air bubble. The Minnaert equation (Minnaert, 1933) was used to determine the resonant frequency (in Hz) for a spherical air bubble and was calculated (using the physical parameters of an air bubble in water just below the ocean surface) from the constant 3.26 divided by the bubble radius (in m). We compared this analytical solution to that predicted by the FEM for two spherical air bubbles, one with a volume equal to the volume of the smallest swim bladder and the other with a volume equal to the volume of the largest swim bladder. Each air bubble was placed in the center of the water sphere with the same excitation previously described. The excitation frequency was swept at increasingly narrow increments to find the maximum response, starting around the Minnaert prediction. The frequency with the highest pressure in the center of the air bubble was considered the resonant frequency. We calculated the percent error of the resonant frequency predicted by the FEM compared with the analytical Minnaert solution.

Determining swim bladder resonant frequency

We imported the swim bladder surfaces for each fish into COMSOL to estimate their resonant frequencies. We performed a search for the resonant frequency by conducting a frequency sweep, in steps of

50 Hz, around the frequency predicted by the Minnaert frequency for a spherical bubble of the same volume. We extracted the amplitude measured at a point in the approximate middle of the bladder, and the frequency with the highest amplitude was considered the resonant frequency. We also performed a wider frequency sweep using three bladders to evaluate their acoustic response to frequencies in the range that is most detectable by fishes. These three bladders were chosen to represent the range of volumes in the sample. We extracted the amplitude measured at the approximate center of the bladders when exposed to plane waves at frequencies of 100–10,000 Hz in steps of 200 Hz.

Acoustic interaction between the swim bladder and otoliths

We used the same FEM environment as described above to investigate whether movement at the otoliths would increase in the presence of a bladder-shaped bubble, and how the magnitude of this motion might change with growth. We did not test hearing thresholds, but rather assumed a direct relationship between predicted pressure sensitivity and the magnitude of modeled motion at the otoliths in the presence of the bubble. For these simulations, we used the STL files that included the six otoliths. We created a linear elastic material representing bone and assigned this to the model otoliths. The acoustic properties of this material (and assigned parameter values) were density (2.7 g ml^{-1}), compressional wave speed (C_p ; 3000 m s^{-1}) and shear wave speed (C_s ; 1400 m s^{-1}). This density was chosen because it is the observed otolith density for red drum larvae reared at the same temperature as our sample fish (Hoff and Fuiman, 1993), and C_p and C_s were chosen as values for bone. We tested the sensitivity of the model to these speed parameters in one fish by comparing the accelerations observed in simulations for a 100 Hz plane wave using $C_p=3000 \text{ m s}^{-1}$ and $C_s=1400 \text{ m s}^{-1}$ with results obtained using the following parameter combinations: keeping density and C_p constant, with C_s at $\pm 50\%$ of the above value; and keeping density and C_s constant, with C_p at $\pm 50\%$ of the above value.

We were most interested in the frequency range to which larval fishes have shown an auditory response (approximately 100–2000 Hz; Wright et al., 2005, 2010, 2011). Red drum have demonstrated sensitivity to frequencies up to 1.2 kHz (Horodysky et al., 2008), while other species have shown responses to test frequencies up to 2 kHz (Wright et al., 2005, 2010, 2011). Within this range, we observed a relatively flat amplitude response in the frequency sweeps compared with the amplitude changes observed around the resonant frequency. Given this observation, we selected four test frequencies to represent the range of bladder responses to frequencies that may be audible to larval fishes, and we introduced a plane wave at 100, 500, 1000 and 2000 Hz at an amplitude of 1 Pa. We extracted the local instantaneous acceleration at four points at the otolith–water boundary, on both left and right pairs (eight points per fish). Points were selected at the otoliths' sulcal grooves, where the sensory maculae are located (Fig. 1).

We re-ran these simulations with the bladder-shaped bubble absent (i.e. model bladder composed of water) to simulate the motion at the otolith–water boundary without the contribution of sound pressure. This is functionally analogous to empirical studies where hearing was tested both before and after bladder deflation (e.g. Yan et al., 2000; Tricas and Boyle, 2015). We extracted the local particle acceleration for the same eight otolith–water boundary points for each fish that we used for the simulations with an air-filled bladder. We calculated a gain factor by dividing the results for the air-filled case by those for the water-filled case, and this ratio was used to compare the predicted contributions of pressure and particle

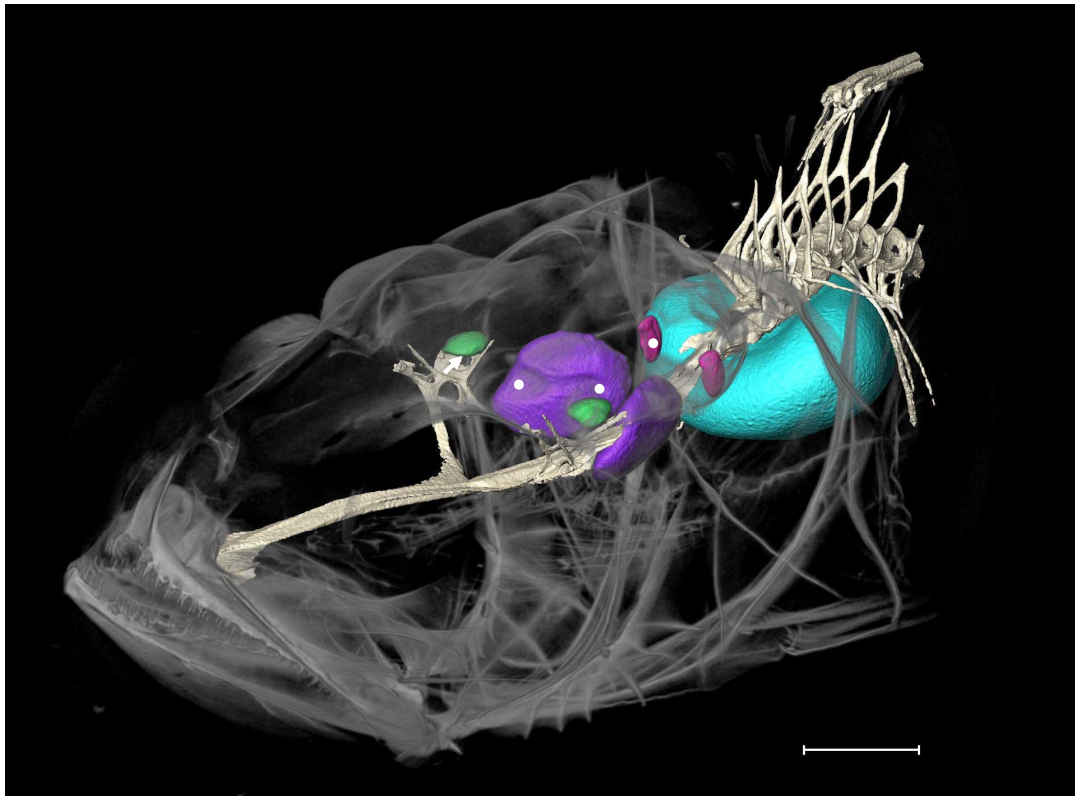


Fig. 1. Otolith and swim bladder morphology in a *Sciaenops ocellatus* larva (9 mm standard length). Micro-computed tomography (microCT) reconstruction showing the position of the otoliths – asterisci (pink), sagittae (purple) and lapilli (green) – relative to the swim bladder (teal). The sulcal grooves on the otolith surface, most visible on the far sagitta, are where the sensory maculae are embedded, which contain the sensory hairs. White dots and arrow indicate the approximate locations on the otolith surface where acceleration values were measured in the finite-element model. Scale bar: 0.5 mm.

motion to audition. A ratio larger than unity was always found, and heretofore this term will be referred to as amplification.

To consider how amplification is influenced by the distance between the otoliths and bladder, we determined the minimum distance between each selected otolith point and its closest point on the anterior face of the swim bladder. In MeshLab, we created a point cloud representation of the bladder surface and exported the three-dimensional coordinates of these points into a custom-written R (v.2.15) script that calculated the distance between each of the eight otolith points and each of the bladder points. The shortest of these distances for each otolith point was plotted against amplification and against SL. To examine how the size of the bladder changes during development, we extracted bladder volume from Avizo and plotted volume against SL. To examine the relationship between the bladder volume and its motion in response to pressure, we plotted the acceleration averaged over the surface of the bladder against volume. Mean surface acceleration was a measurement extracted from COMSOL Multiphysics.

Testing the influence of the vertebrae and ribs on swim bladder motion

MicroCT imagery showed that some of the vertebrae and ribs pressed into the swim bladder (Figs 1 and 2), possibly reducing movement of the swim bladder in response to pressure fluctuations. The surfaces of these bones were not included in the simulations because of the high computational demand; rather, we created idealized, or representative, geometry to simulate these bony elements to test the potential influence of the comparatively rigid structures of the backbone and first three ribs on the movement of

the bladder. The first three ribs were consistently observed to imprint on the bladder surface in the microCT imagery. The microCT imagery supported the findings of Kubicek and Conway (2016) that the ribs are one of the final bones to calcify; the smallest fish (8.5 mm) had only partially calcified ribs compared with the entirely calcified ribs of the larger individuals. If the ribs impede bladder motion, it would most likely occur in larger fish with calcified ribs rather than in smaller fish with ribs of more flexible cartilage. The 14 mm SL fish had well-calcified ribs, and we used this fish to model the idealized geometry. The bladder was idealized as a prolate spheroid with a volume and length matching those of the observed bladder. The vertebrae and ribs were represented by cylinders that approximated the dimensions of these structures and were assigned the same acoustic properties as the otoliths. We ran three simulations to test the effect of these solid structures on bladder movement: (1) idealized swim bladder only, (2) idealized swim bladder plus vertebrae and (3) idealized swim bladder plus vertebrae and ribs. We introduced a plane wave at 100 Hz and measured the instantaneous local acceleration at a point 1 mm anterior to the face of the swim bladder. We compared this value among the three simulations. We also compared the amplitude measured at the approximate center of both the idealized bladder and the bladder from the 14 mm SL fish to test the appropriateness of the prolate spheroid as a replica for the actual bladder.

RESULTS

Ontogenetic change in larval fish morphology

Swim bladder volume increased allometrically with standard length (allometric coefficient=3.06, $R^2=0.79$; Figs 2 and 3A). Swim

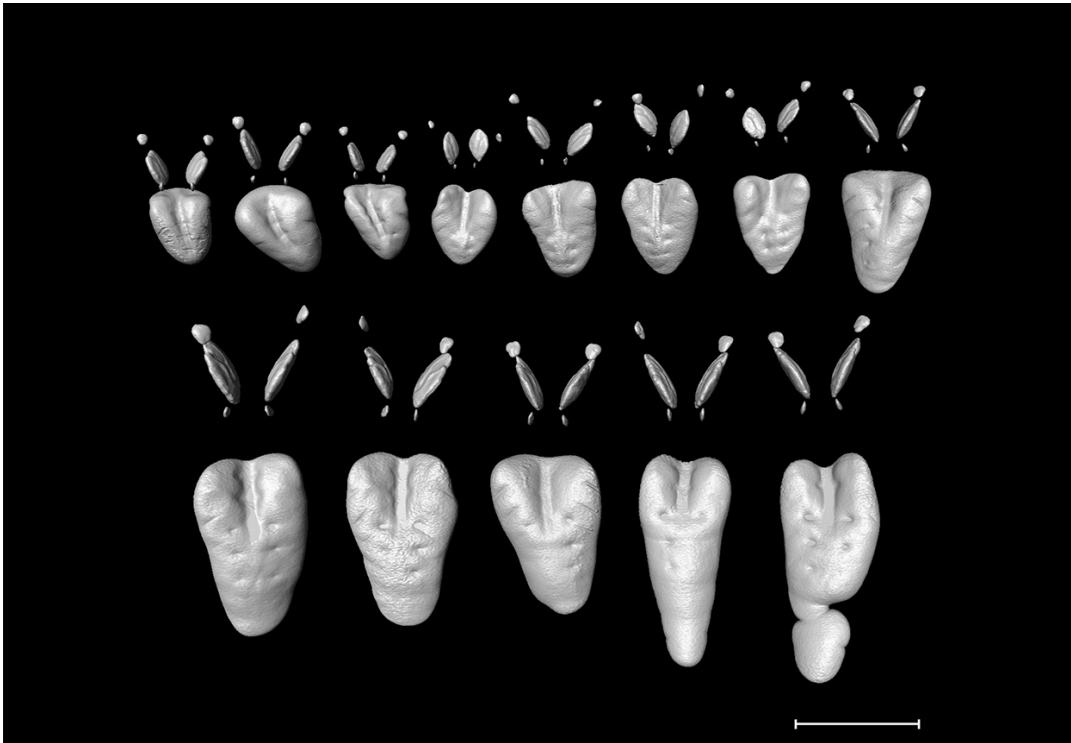


Fig. 2. Ontogenetic change in *S. ocellatus* swim bladder and otolith morphology. MicroCT reconstruction of the swim bladder and otoliths from 13 larvae that ranged in size from 8.5 to 18 mm standard length (SL). Fish are arranged by size from smallest in the top row, far left, to largest in the bottom row, far right. Note the increasing distance between the otoliths and bladder with fish length, and indentations of vertebrae and ribs on the bladders. Scale bar: 2 mm.

bladder volumes ranged from 0.26 to 2.7 mm³. The minimum distance between selected points on the otolith surface and the swim bladder increased linearly with the standard length of the fish (Fig. 4). There was left–right asymmetry in these distances, i.e. there were differences in the measurements between the left and right otolith pairs, but neither side was consistently closer to or farther from the bladder. Mean (\pm s.d.) asymmetry for the asterisci, sagittae and lapilli, respectively, was: 0.039 \pm 0.026, 0.077 \pm 0.06 and 0.13 \pm 0.095 mm. Across all fish, the minimum distance between the selected point on the otolith and its closest point on the bladder ranged from 0.11 to 0.99 mm for the asterisci, 0.22 to 1.63 mm for the posterior sagittae, 0.46 to 2.18 mm for the anterior sagittae, and 0.74 to 2.52 mm for the lapilli.

Modeled acoustic response of the swim bladder

There was an inverse relationship between swim bladder resonant frequency and volume (Fig. 5). Modeled resonant frequencies ranged from 4250 Hz for the largest bladder (by volume) to 8750 Hz for the smallest bladder. In the frequency sweeps, the amplitude remained relatively unchanged until the resonant frequency was approached, at which point the pressure rapidly increased and peaked (Fig. 6). The acceleration averaged over the surface of the swim bladder increased linearly with bladder volume (Fig. 3B).

The analytical solution for the resonant frequency of a spherical air bubble with a volume equal to that of the largest bladder was 3790 Hz, compared with the FEM solution of 3820 Hz (0.79% error; Fig. 5). The analytical solution for the resonant frequency of a spherical bubble matching the volume of the smallest bladder was 8150 Hz, compared with the FEM solution of 8212 Hz (0.76% error; Fig. 5). These results support the ability of the model to simulate the acoustic behavior of the bladder-shaped bubble and its

interaction with the model otoliths. In both cases, the resonant frequency for the spherical bubble was lower than the resonant frequency observed for the bladder-shaped bubble of matching volume.

Modeled acoustic interaction between swim bladder and otoliths

Modeled acceleration at selected points on the otolith–water boundaries due to the presence of the bladder-shaped bubble decreased with increasing otolith–bladder distance (Fig. 7). At 100 Hz, amplification values across otolith points ranged from 54 to 3485, demonstrating the contribution of the bladder-shaped bubble to simulated motion at the otoliths. There was a small increase in amplification with increasing test frequency. Across all fish and using all eight otolith points for each fish, the mean (\pm s.d.) percentage increase in amplification for the other test frequencies relative to the values at 100 Hz was: 0.76 \pm 0.03% at 500 Hz, 3.2 \pm 0.03% at 1000 Hz and 12.8 \pm 0.03% at 2000 Hz. The shape of the relationship between amplification and otolith–bladder distance (Fig. 7) remained consistent across test frequencies.

Within a fish, amplification values were highest at the points on the asterisci and second highest at the points on the posterior sagitta. Fish geometries with smaller bladder volumes and otolith–bladder distances had the greatest amplification (Fig. 8). In general, amplification decreased with increasing otolith–bladder distance in fish with bladders of a similar size (see Fig. 8 for bladder volumes <0.6 mm³). Increasing swim bladder volume appeared to partially compensate for this loss in amplification. That is, there were instances of a greater amplification in fish with bladder volumes >1 mm³ compared with that in fish with bladders <0.6 mm³, despite the larger fish having greater otolith–bladder distance (Fig. 8).

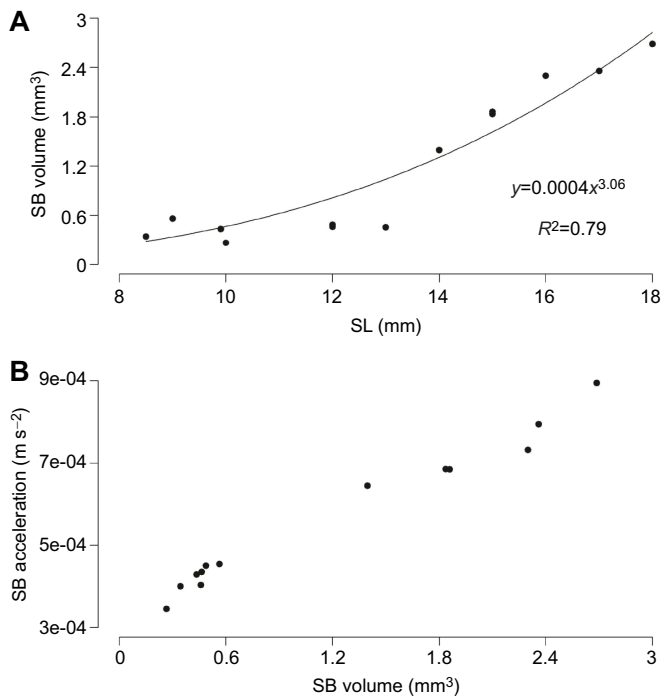


Fig. 3. Ontogenetic change in *S. ocellatus* swim bladder properties. (A) Swim bladder (SB) volume increased allometrically with SL for the study fish ($n=13$). Volumes for the two 12 mm SL fish and the two 15 mm SL fish overlap. (B) Swim bladder acceleration averaged across the surface of the swim bladder increased with swim bladder volume. Data from a finite-element model of a 1 Pa, 100 Hz plane wave laterally approaching the bladder.

Sensitivity analysis showed little effect of changes in C_s and C_p on acceleration.

Modeled influence of the vertebrae and ribs on swim bladder motion

The idealized bladder and the bladder geometry obtained from the microCT imagery (Fig. 9) responded similarly to plane waves at 100, 500, 1000 and 2000 Hz. The percentage difference in absolute amplitude measured in the center of these two geometries was 0%, 0.03%, 0.16% and 0.70%, respectively. When the vertebrae were added to the idealized bladder, the acceleration at a point 1 mm anterior to the bladder decreased by 5.4%, 5.3%, 5.3% and 5.2% at the respective test frequencies. When the vertebrae and ribs were added, there was a 5.1%, 5.1%, 5.0% and 4.9% decrease in acceleration at 100, 500, 1000 and 2000 Hz, respectively, compared with that for the idealized bladder alone.

DISCUSSION

We investigated the ontogenetic changes in morphological features likely to influence a fish's ability to detect the pressure component of sound by using a combination of microCT imagery and FEM. In all fish and across all otoliths, the amplification was non-zero, and much greater than zero at the otoliths closest to the bladder that are predicted to play a role in pressure sensitivity (Braun and Grande, 2008; Schultz-Mirbach et al., 2013). We originally hypothesized an ontogenetic decrease in indirect stimulation at the otoliths resulting from increasing otolith–bladder distance. While we did observe these distances to increase with standard length, amplification values obtained from the model did not decrease monotonically with increasing fish size. Predicted pressure sensitivity was highest in the smaller fish, but growth in bladder volume helped larger

larvae regain simulated amplification that was lost as a result of increasing distance, suggesting sound pressure may be a usable stimulus throughout the larval stage.

Ontogenetic changes in predicted pressure sensitivity

The presence of an air bubble and its proximity to the otic capsule determines where a fish species falls along the proposed continuum of pressure sensitivity relative to particle motion (Popper and Fay, 2011). At one end of this continuum are species with a mechanical connection between the bladder and otic capsule that enables high sensitivity to pressure. On the other end are species with no swim bladder and no pressure sensitivity, using just particle motion for sound detection. In between are fishes with varying degrees of pressure sensitivity as determined by the distance between the bladder and otoliths and the presence of ancillary hearing structures (Popper and Fay, 2011; Radford et al., 2012). Applied to the intraspecific case, this framework leads to the hypothesis for larval fishes of an ontogenetic decrease in indirect stimulation of the otoliths resulting from increasing otolith–bladder distance as larvae grow. Our measurements confirmed that otolith–bladder distance increased with standard length in red drum and our modeling results show that amplification of acoustic pressure at the otoliths decreased as otolith–bladder distance increased. In the model, larvae with similar bladder volumes (<0.6 mm³; Fig. 8) showed decreasing amplification with increasing otolith–bladder distance. These results support previous studies that observed ontogenetic decreases in auditory sensitivity and speculated that ontogenetically increasing distances between the bladder and inner ear was a potential cause (Egner and Mann, 2005; Colley et al., 2016). At larger fish sizes, the ontogenetically increasing bladder volume appeared to partially compensate for the amplification loss produced by greater otolith–bladder distance. This is demonstrated by observations that some individuals with bladder volumes >0.6 mm³ showed greater simulated amplification than some individuals with smaller otolith–bladder distances but also smaller bladders (Fig. 8). This partial recovery of pressure sensitivity may allow bladder volume, while not a specific auditory adaptation, to have a functional effect similar to increasing hair cell density (Rogers et al., 1988; Higgs et al., 2002) or developing anterior bladder extensions (Webb et al., 2012). We predict that the ontogenetic changes in otolith–bladder distance and bladder size may result in a non-linear ontogenetic change in pressure sensitivity, potentially altering how larvae perceive sounds in their environment.

Implications of the acoustic response of the bladder to audition

The frequency sweeps demonstrated that the amplitude of simulated bladder pulsation is low at frequencies that larvae of red drum and other species hear best (100–300 Hz; Horodysky et al., 2008; Wright et al., 2011; Havel, 2014). Despite this, we observed that the bladder amplitudes at 100 Hz amplified the plane wave stimulus by 54–3485 times, and we predict the bladder may enable pressure sensitivity at the low frequencies that are important to larvae but far from the resonant frequency. There was an indirect relationship between bladder volume and the resonant frequency estimated by the model, as predicted by the Minnaert equation. Amplification increased with the frequency of the plane wave, and amplification values at the highest frequency tested (2000 Hz) were, on average, approximately 13% greater than those observed at the lowest test frequency (100 Hz). This is to be expected, because predicted resonant frequencies of the bladders were greater than the test frequencies. The closer the plane wave frequency was to the bladder

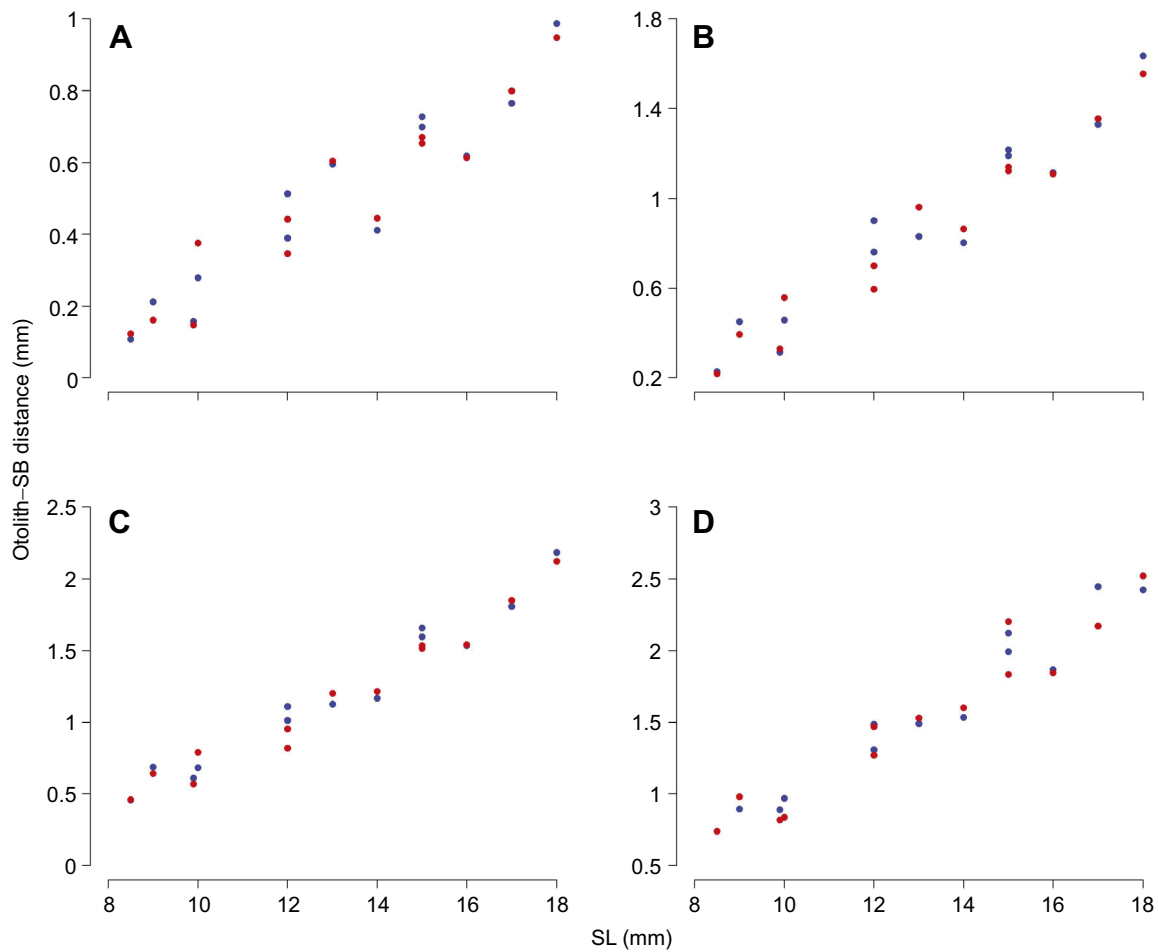


Fig. 4. Ontogenetic change in *S. ocellatus* otolith–swim bladder distance. (A) Asterisci, (B) posterior sagittae, (C) anterior sagittae and (D) lapilli. Color identifies left (blue) and right (red) otoliths for each pair in each fish ($n=13$).

resonant frequency, the greater the amplitude of bladder pulsations and the greater the pressure-produced particle motion propagating towards the otoliths. This supports the notion that pressure may have an unequal contribution to hearing across the audible frequency range – the relative strength of indirect stimulation compared with direct stimulation may increase as the frequency of a sound gets closer to the bladder’s resonant frequency. This is supported by the higher audible frequency range in fishes that have a greater sensitivity to pressure (Ramcharitar et al., 2006b). Further, our results support the prediction that bladder size influences the maximum audible frequency (as observed in Egner and Mann, 2005; Schultz-Mirbach et al., 2012). The larger bladders in our simulation showed both higher surface acceleration (Fig. 3B) and a greater amplitude of motion as the test frequency got closer to the resonant frequency (Fig. 6). Thus, while bladders of all sizes will have a greater amplitude when exposed to frequencies closer to their resonant frequency, the additional contribution of the greater surface acceleration of a larger bladder may help to increase the sensitivity of fish to frequencies above the range of best detection (Braun and Grande, 2008).

In considering the implications of bladder resonance for fish hearing, it is important to remember that our model includes only the swim bladder and otolith geometries in a sphere of water, leaving out the muscles and other tissues that will influence the cumulative response of the bladder to acoustic stimuli (e.g.

McCartney and Stubbs, 1971; Sand and Hawkins, 1973; Fine et al., 2016). Tissues between the bladder and otoliths that have a viscosity greater than that of water would dampen the energy received at the otoliths from the bladder (Love, 1978; Feuillade and Nero, 1998), thus reducing the magnitude of the effect we observed. Further, properties of the adult bladder wall can prevent it from acting as a resonant structure, drawing into question the appropriateness of modeling swim bladders as resonant bubbles (Fine, 2012; Fine et al., 2016). However, here we were interested in the larval stage; in the larval condition, swim bladders are thin-walled, even in species of chaetodontids and cichlids that have a thick tunica externa as adults (J. F. Webb, University of Rhode Island, personal communication). These observations of ontogenetic differences in bladder wall structure suggest that modeling the larval bladder with a bubble is more appropriate than for the adult bladder, supporting our interpretations. Our results indicate that the vertebrae and ribs have minimal influence on bladder motion, and this is supported by the ribs contacting only a relatively small area of the dorsal and dorsolateral bladder, and they have no direct effect on the vibrations of the anterior, lateral and ventral bladder. The greater calcification of the ribs of larger fish should not alter our predictions of relative pressure sensitivity between the fish. Further, the weak effect of these rigid structures suggests that additional ribs that attach to the bladder beyond those tested are also unlikely to significantly impede bladder motion.

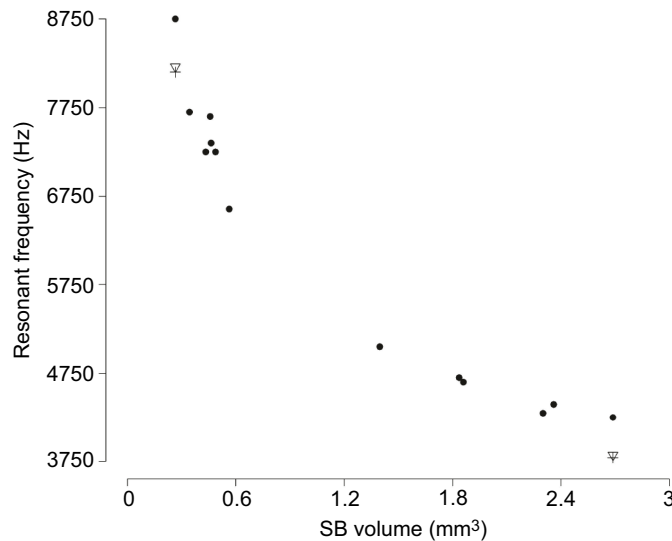


Fig. 5. Variation in modeled swim bladder resonant frequency with swim bladder volume. The filled circles represent the model-predicted resonant frequencies of the swim bladders of the study fish ($n=13$). Inverted triangles represent the resonant frequencies predicted by the model for spherical air bubbles that matched the volumes of the smallest and largest bladders. Crosses represent the analytical solution for these same spherical bubbles using the Minnaert equation. The similarity in the predicted values and analytical solution (<1% error) supports the use of this model to predict the acoustic behavior of the fish geometry.

Interspecific comparisons of otolith–bladder distance conducive to indirect stimulation

We used accelerations obtained by FEM to calculate a relative term of amplification to measure the contribution of indirect stimulation (via the bladder) compared with direct stimulation (via the plane wave) to simulated motion at the selected otolith points. We did not compare model-derived accelerations with thresholds needed to stimulate a hair cell (e.g. Fay and Simmons, 1999) given our simplified model of the fish. We instead assumed a direct relationship between amplification and the likelihood of indirect stimulation at the otoliths. It is therefore relevant to ask whether the

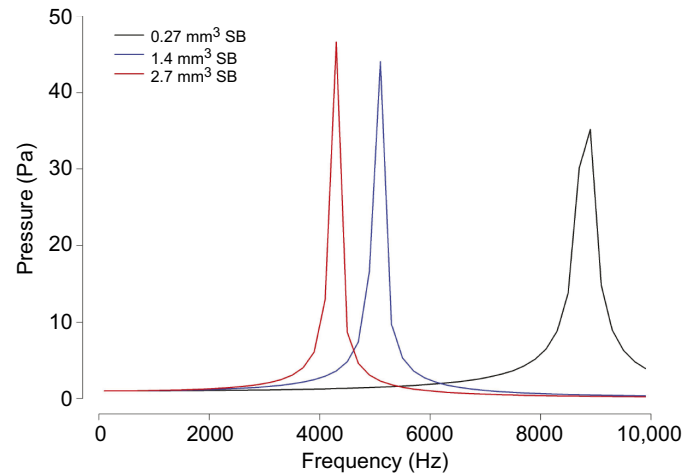


Fig. 6. Modeled acoustic behavior of swim bladders. Frequency sweeps (100–10,000 Hz, in steps of 200 Hz) were conducted on bladders chosen to represent the range of swim bladder sizes observed in the study fish. A bladder's resonant frequency was determined to be the approximate frequency at which the maximum pressure amplitude occurred, and this frequency increased with decreasing bladder volume.

otolith–bladder distance observed in larval red drum allows these fish to use the pressure component of sound. This distance combined with the magnitude of bladder motion are key factors in whether and to what degree a fish will detect acoustic pressure. In a larval swim bladder with a thin bladder wall, the motion of the bladder in response to acoustic pressure will be greatest at that bladder's resonant frequency. Given the small size of larvae, resonant frequencies are greater than a fish's maximum audible frequency. However, there may still be sufficient motion of the larval bladder at frequencies even below resonance to indirectly stimulate the otoliths, given a sufficiently small bladder–otolith distance.

Adult *Paratilapia polleni* and *Ectoplos maculatus* have anterior bladder extensions terminating within 1 mm of the inner ear and higher auditory sensitivity compared with that of two species (*Hemichromis guttatus* and *Steatocranus tinanti*) with a greater

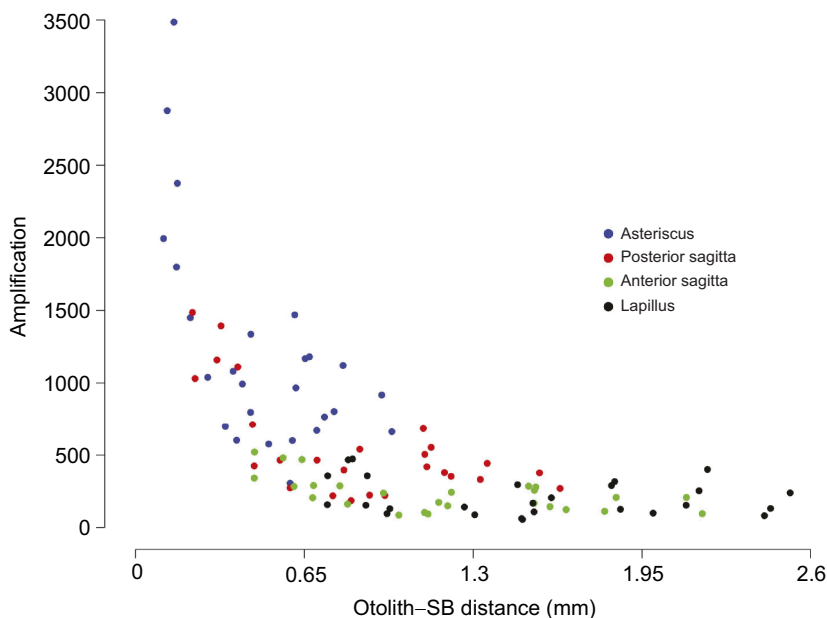


Fig. 7. Relationship between otolith–swim bladder distance and modeled amplification by acoustic pressure at the otoliths. Amplification is the ratio of indirect and direct stimulation at selected points on the surface of the otolith (as shown in Fig. 1). Otolith–swim bladder distance is the shortest distance between these points and the bladder (Fig. 4). Results are shown for a 1 Pa acoustic stimulus at 100 Hz. Relationships were similar at the other test frequencies (500, 1000 and 2000 Hz), but shifted along the y-axis. More amplification was observed at higher frequencies because they were closer to bladder resonant frequency. Data from simulations using morphology from 13 larvae, and eight points of measurement per fish (left and right otoliths).

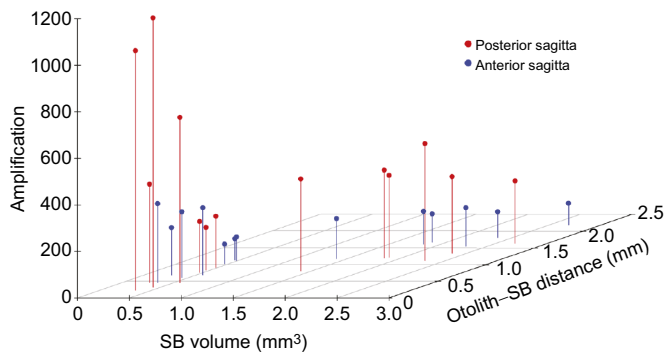


Fig. 8. Relationship between modeled amplification and bladder volume and otolith–swim bladder distance for the sagitta otolith. Amplification is the ratio of indirect and direct stimulation at selected points on the surface of the otolith. Otolith–swim bladder distance is the shortest distance between these points and the bladder (Fig. 4). Points on the anterior and posterior ends of the sulcal groove (Fig. 1) were measured for the sagittal otoliths for each fish ($n=13$). Data for the left sagitta otolith are shown.

distance between the inner ears and bladder (Schultz-Mirbach et al., 2012). In a study comparing two sciaenid species (the family including red drum), *Micropogonias undulatus* showed more resistance to threshold shifts from masking than did *Pogonias chromis*; *M. undulatus* has anterior bladder extensions ending at a mean distance of 3.8 mm from the otic capsule, compared with a mean distance of 7.4 mm in *P. chromis* (Ramcharitar and Popper, 2004). Ramcharitar et al. (2006b) compared the maximum detectable frequency with otic capsule–bladder distance across six sciaenid species, showing an apparent exponential decline in the maximum frequency with increasing distance (a trend similar to that in Fig. 7). *Bairdiella chrysoura*, with an average otic capsule–bladder distance of approximately 1.6 mm, had a maximum detectable frequency up to 4 kHz. Distances less than 4 mm appeared to increase the maximum detectable frequency above that generally expected from particle motion alone (Braun and Grande, 2008), which was observed for species with a mean otic capsule–bladder distance >7 mm. These distances are similar to those observed for *Opsanus tau* and *Trichogaster trichopterus* (6–8 mm) for which removal of the bladder had no significant effect on hearing thresholds (Yan et al., 2000), suggesting pressure-generated particle motion is severely attenuated over these distances. Looking across these studies, fishes with distances approaching 1 cm had less, or no, influence from the bladder, compared with that for fishes with distances <0.5 cm. Propagation of pressure-generated particle motion appears to be most effective over otolith–bladder distances <1 mm. This is supported by observations of larval *Chaetodon ocellatus*, for which the development of anterior bladder extensions maintained an otolith–bladder distance <1 mm during development, and this was predicted to maintain pressure sensitivity (Webb et al., 2012).

We measured otolith–bladder distance from each otolith point to its nearest point on the bladder. This is different from the aforementioned studies that measured the distance between the swim bladder and otic capsule or the closest posterior otolith edge. Despite this, all of our distances were <2.5 mm and many were <1 mm (Fig. 4). Comparing these simulation results with results from other studies leads us to predict that there is sufficient pressure-produced particle motion in red drum larvae (8–18 mm SL) to reach the otoliths and improve hearing capability. The position of the different otoliths relative to the bladder suggests they contribute differently to sound pressure detection. All larvae had distances

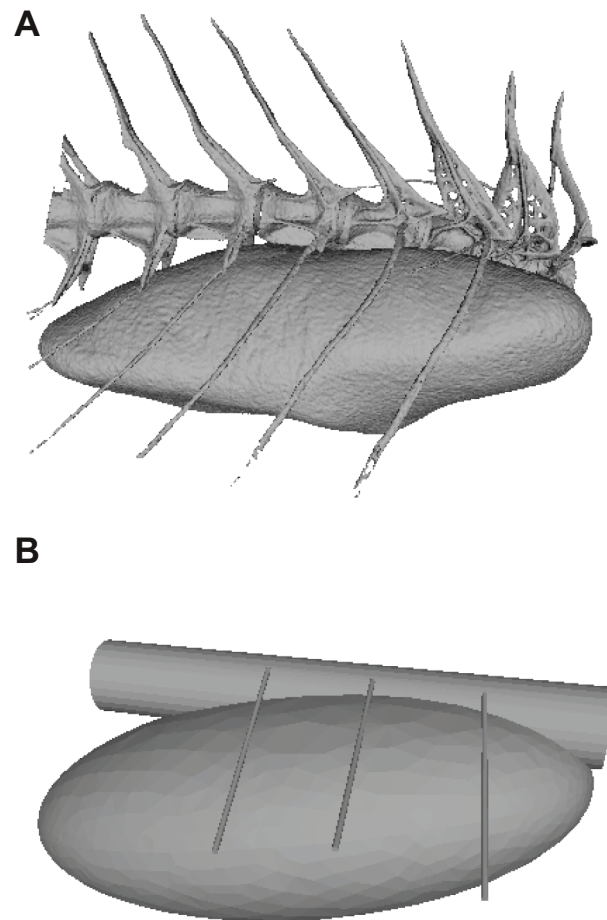


Fig. 9. Testing the effect of the vertebrae and ribs on bladder motion. (A) MicroCT reconstruction of spine–bladder morphology and (B) its idealized geometry. Model results using the idealized geometry predict that the vertebrae and ribs have minimal influence on the re-radiated pressure stimulus. Features in A were extracted from a 14 mm SL larva and served as the model for this test.

<1 mm between the bladder and asterisci, and all otoliths were within this distance in the smallest fish. The specific functions of the different pairs of otoliths is species specific and not fully known (Popper and Schilt, 2008); however, the sagittae and asterisci are thought to have specific auditory functions and are the likely receptors of pressure-produced particle motion (Braun and Grande, 2008; Schultz-Mirbach et al., 2013). The points on the asterisci and posterior sagittae were closest to the bladder and had the greatest modeled amplification, supporting their role in pressure detection in larvae. The auditory consequence, if any, of the left–right asymmetry in otolith–bladder distance is unknown. This result may be partly due to slight bending of the fish during the CT scan, but the observed position of the fish before and after the scans supports that the body of the larvae remained relatively straight.

Potential implications of larval pressure sensitivity for settlement behavior

Until we have a better understanding of the relative roles of direct (via particle motion) and indirect (via pressure) stimulation of otoliths in larval fish hearing, particle motion should not be assumed to be the only acoustic stimulus for larvae in an ecological setting, as suggested in recent literature (e.g. Mann et al., 2007;

Kaplan and Mooney, 2016; Nedelec et al., 2016). In our modeling, the morphology of red drum larvae produced a significant increase in the amplification of the acoustic stimulus at the otoliths in the presence of the bladder. This occurred even at frequencies far below predicted bladder resonance. Thus, even without an otophysic connection or special adaptation of the bladder (e.g. anterior extensions, auditory bulla), larvae of many species of fishes may be equipped to sense pressure in addition to particle motion once the bladder fills with air.

Detecting the pressure component of sound would be extremely valuable to species with larvae that use acoustic cues during the settlement process. Benthic habitats have distinct soundscapes (Radford et al., 2010; Lillis et al., 2014; Butler et al., 2016) and these habitat-specific sound signatures may assist larval fishes in locating and selecting preferred habitat types (Simpson et al., 2008; Parmentier et al., 2015; Gordon et al., 2018). The distance at which fishes detect acoustic cues from their sources is important when considering both the function of these sounds (e.g. habitat selection at close range, navigation at long range, or both) and the degree to which they may improve settlement success (Codling et al., 2004). The fundamental question in determining whether a larva can detect either the particle motion or pressure component of a potential cue is whether the amplitude of the acoustic stimulus is greater than the fish's detection threshold (and greater than the ambient noise level). As pressure sensitivity decreases auditory thresholds (Parmentier et al., 2011; Schultz-Mirbach et al., 2012; Tricas and Boyle, 2015), acoustic cues are more likely to be detected by larvae at a distance from sound sources if the fish are capable of using pressure. Further, the perception of acoustic pressure is thought to be necessary for localizing sound sources (Schuijf and Hawkins, 1983), an ability demonstrated by some larval fishes (Tolimieri et al., 2004; Leis and Lockett, 2005). Lastly, the extended frequency range enabled by pressure detection (Ramcharitar et al., 2006b) would allow more frequency components of a habitat's soundscape to function as cues for larvae that can use pressure. This extended frequency range would increase detection of the higher frequency components of coastal soundscapes to which larvae may be attracted (Simpson et al., 2008). Higher frequencies also produced more bladder motion in the model as they are closer to bladder resonance, leading to greater amplification. In this study, our measurements and modeling support the potential for pressure sensitivity in larval fishes, enabled simply by their small size creating short bladder–otolith distances. The results of previous studies support the importance of acoustic cues during settlement for some species of larval fishes. Pressure sensitivity expands the utility of the soundscape to these fishes – with this ability, more sounds in a habitat's soundscape will have the necessary amplitude and frequency characteristics to be detected and potentially used to improve the probability of successful settlement.

Conclusions

A sound in the environment has particle motion and pressure components, and an ability to use both components makes available to a fish additional sensory information compared with particle motion detection alone. There are species-level differences in a fish's ability to use the pressure component of sound and the degree to which pressure contributes to hearing. These differences are primarily attributed to the presence of a bladder and the distance over which pressure-produced particle motion must propagate to reach the otoliths. If the distance is too great relative to the strength of the particle motion, the motion will attenuate before reaching the inner ear. Similarly, ontogenetic change in the distance between the

bladder and otoliths suggests larvae at different developmental stages will vary in how much their hearing is influenced by indirect or direct stimulation. We observed differences in otolith–bladder distance and bladder size across the developmental stages of red drum, and both of these features influenced model-predicted pressure sensitivity. Considering these two features alone, the smaller fish in our study would be more likely to use the pressure component of a sound to improve hearing. While this capacity may decrease with growth, increases in bladder volume may offset some of the loss in pressure amplification. It is likely there is some otolith–bladder distance threshold over which increasing bladder volume could not compensate. We expect that our predictions apply to other species in which the larval bladder is close to the otoliths. Bladder volume increases with fish growth, and an increase in otolith–bladder distance is expected, except in species where this is mitigated by specialized adaptations. As pressure sensitivity affects how environmental sounds are perceived, in terms of both frequency range and detection distance, ontogenetic changes in the use of sound pressure would dynamically influence how acoustic cues and signals are used during the larval stage. Sound is a key sensory modality in the underwater environment, and a fish's sensitivity to pressure enables sound detection at greater distances, the ability to sense a broader range of frequencies and improved sound localization; how this capability changes over the course of early development has implications for settlement success and survival.

Acknowledgements

We thank Cindy Faulk, Dr Ken Webb and Zhenxin Hou for larval rearing and help with collecting and preparing the study fish. We thank Zhenxin Hou for help with the description of the rearing methods. We thank Drs Jessica Maisano and Matthew Colbert for lending their expertise to the microCT scanning and image preparation, and Dr Anthony Bonomo for his assistance with the finite-element modeling. We thank Dr Michael Fine for his recommended revisions, which improved the manuscript.

Competing interests

The authors declare no competing or financial interests.

Author contributions

Conceptualization: A.K.S., P.S.W., L.A.F.; Methodology: A.K.S., P.S.W., L.A.F.; Software: A.K.S.; Validation: A.K.S.; Formal analysis: A.K.S., L.A.F.; Investigation: A.K.S., L.A.F.; Resources: A.K.S., P.S.W., L.A.F.; Data curation: A.K.S.; Writing - original draft: A.K.S.; Writing - review & editing: A.K.S., P.S.W., L.A.F.; Visualization: A.K.S., P.S.W., L.A.F.; Supervision: P.S.W., L.A.F.; Project administration: A.K.S., P.S.W., L.A.F.; Funding acquisition: A.K.S., P.S.W., L.A.F.

Funding

This work was supported by the American Museum of Natural History Lerner Gray Fund for Marine Research (to A.K.S.), the Perry R. Bass Endowment at the University of Texas Marine Science Institute (to L.A.F.), and the Office of Naval Research Ocean Acoustics Program (grant number N00014-15-1-2032 to P.S.W.).

References

- Atema, J., Gerlach, G. and Paris, C. B.** (2015). Sensory biology and navigation behavior of reef fish larvae. In *Ecology of Fishes on Coral Reefs* (ed. C. Mora), pp. 3-15. Cambridge: Cambridge University Press.
- Blaxter, J. H. S. and Fuiman, L. A.** (1990). The role of the sensory systems of herring larvae in evading predatory fishes. *J. Mar. Biol. Ass. U.K.* **70**, 413-427. doi:10.1017/S0025315400035505
- Braun, C. B. and Grande, T.** (2008). Evolution of peripheral mechanisms for the enhancement of sound reception. In *Fish Bioacoustics* (ed. J. F. Webb, R. R. Fay and A. N. Popper), pp. 99-144. New York: Springer Publishing.
- Butler, J., Stanley, J. A. and Butler, M. J.** (2016). Underwater soundscapes in near-shore tropical habitats and the effects of environmental degradation and habitat restoration. *J. Exp. Mar. Biol. Ecol.* **479**, 89-96. doi:10.1016/j.jembe.2016.03.006

- Codling, E. A., Hill, N. A., Pitchford, J. W. and Simpson, S. D.** (2004). Random walk models for the movement and recruitment of reef fish larvae. *Mar. Ecol. Prog. Ser.* **279**, 215–224. doi:10.3354/meps279215
- Colleye, O., Kéver, L., Lecchini, D., Berten, L. and Parmentier, E.** (2016). Auditory evoked potential audiograms in post-settlement stage individuals of coral reef fishes. *J. Exp. Mar. Biol. Ecol.* **483**, 1–9. doi:10.1016/j.jembe.2016.05.007
- Cranford, T. W. and Krysl, P.** (2015). Fin whale sound reception mechanisms: skull vibration enables low-frequency hearing. *PLoS ONE* **10**, e0116222. doi:10.1371/journal.pone.0116222
- Cranford, T. W., Krysl, P. and Amundin, M.** (2010). A new acoustic portal into the Odontocete ear and vibrational analysis of the Tympanoperiotic complex. *PLoS ONE* **5**, e11927. doi:10.1371/journal.pone.0011927
- Egner, S. A. and Mann, D. A.** (2005). Auditory sensitivity of sergeant major damselfish *Abudefduf saxatilis* from post-settlement juvenile to adult. *Mar. Ecol. Prog. Ser.* **285**, 213–222. doi:10.3354/meps285213
- Fay, R. R. and Simmons, A. M.** (1999). The sense of hearing in fishes and amphibians. In *Comparative Hearing: Fish and Amphibians* (ed. R. R. Fay and A. N. Popper), pp. 269–318. New York: Springer Publishing.
- Feuillade, C. and Nero, R. W.** (1998). A viscous-elastic swimbladder model for describing enhanced-frequency resonance scattering from fish. *J. Acoust. Soc. Am.* **103**, 3245–3255. doi:10.1121/1.423076
- Fine, M. L.** (2012). Swimbladder sound production: the forced response versus the resonant bubble. *Bioacoustics* **21**, 5–7. doi:10.1080/09524622.2011.647453
- Fine, M. L., King, T. L., Ali, H., Sidker, N. and Cameron, T. M.** (2016). Wall structure and material properties cause viscous damping of swimbladder sounds in the oyster toadfish *Opsanus tau*. *Proc. Roy. Soc. Lond. B.* **283**, 1–9. doi:10.1098/rspb.2016.1094
- Fuiman, L. A.** (1989). Vulnerability of Atlantic herring larvae to predation by yearling herring. *Mar. Ecol. Prog. Ser.* **51**, 291–299. doi:10.3354/meps051291
- Gordon, T. A. C., Harding, H. R., Wong, K. E., Merchant, N. D., Meekan, M. G., McCormick, M. I., Radford, A. N. and Simpson, S. D.** (2018). Habitat degradation negatively affects auditory settlement behavior of coral reef fishes. *Proc. Nat. Acad. Sci. USA* **115**, 5193–5198. doi:10.1073/pnas.1719291115
- Havel, L. N.** (2014). Habitat selection: How sensory systems influence settlement patterns in larval red drum (*Sciaenops ocellatus*). *PhD thesis*, The University of Texas at Austin, Austin, Texas.
- Havel, L. N. and Fuiman, L. A.** (2016). Settlement-size larval red drum (*Sciaenops ocellatus*) respond to estuarine chemical cues. *Estuaries Coasts* **39**, 560–570. doi:10.1007/s12237-015-0008-6
- Havel, L. N., Fuiman, L. A. and Ojanguren, A. F.** (2015). Benthic habitat properties can delay settlement in an estuarine fish (*Sciaenops ocellatus*). *Aquat. Biol.* **24**, 81–90. doi:10.3354/ab00639
- Higgs, D. M., Souza, M. J., Wilkins, H. R., Presson, J. C. and Popper, A. N.** (2002). Age- and size-related changes in the inner ear and hearing ability of the adult Zebrafish (*Danio rerio*). *J. Assoc. Res. Oto.* **3**, 174–184. doi:10.1007/s101620020035
- Hoff, G. R. and Fuiman, L. A.** (1993). Morphometry and composition of red drum otoliths: changes associated with temperature, somatic growth rate, and age. *Comp. Biochem. Physiol.* **106**, 209–219. doi:10.1016/0300-9629(93)90502-U
- Horodysky, A. Z., Brill, R. W., Fine, M. L., Musick, J. A. and Latour, R. J.** (2008). Acoustic pressure and particle motion thresholds in six sciaenid fishes. *J. Exp. Biol.* **211**, 1504–1511. doi:10.1242/jeb.016196
- Ihlenburg, F.** (1998). *Finite Element Analysis of Acoustic Scattering*. New York: Springer Publishing.
- Kaplan, M. B. and Mooney, T. A.** (2016). Coral reef soundscapes may not be detectable far from the reef. *Sci. Rep.* **6**, 31862. doi:10.1038/srep31862
- Kenyon, T. N.** (1996). Ontogenetic changes in the auditory sensitivity of damselfish (Pomacentridae). *J. Comp. Physiol. A* **179**, 553–561. doi:10.1007/BF00192321
- Kubicek, K. M. and Conway, K. W.** (2016). Developmental osteology of *Sciaenops ocellatus* and *Cynoscion nebulosus* (Teleostei: Sciaenidae), economically important sciaenids from the western Atlantic. *Acta Zool-Stockholm* **97**, 267–301. doi:10.1111/azo.12122
- Leis, J. M. and Lockett, M. M.** (2005). Localization of reef sounds by settlement-stage larvae of coral-reef fishes (Pomacentridae). *Bull. Mar. Sci.* **76**, 715–724.
- Lillis, A., Eggleston, D. B. and Bohnenstiehl, D. R.** (2014). Estuarine soundscapes: distinct acoustic characteristics of oyster reefs compared to soft-bottom habitats. *Mar. Ecol. Prog. Ser.* **505**, 1–17. doi:10.3354/meps10805
- Love, R. H.** (1978). Resonant acoustic scattering by swimbladder-bearing fish. *J. Acoust. Soc. Am.* **64**, 571–580. doi:10.1121/1.382009
- Mann, D. A., Casper, B. M., Boyle, K. S. and Tricas, T. C.** (2007). On the attraction of larval fishes to reef sounds. *Mar. Ecol. Prog. Ser.* **338**, 307–310. doi:10.3354/meps338307
- McCartney, B. S. and Stubbs, A. R.** (1971). Measurements of the acoustic target strengths of fish in dorsal aspect, including swimbladder resonance. *J. Sound. Vib.* **15**, 397–420. doi:10.1016/0022-460X(71)90433-0
- Minnaert, M.** (1933). On musical air-bubbles and the sounds of running water. *Lond. Edinb. Dublin Philos. Mag. J. Sci.* **16**, 235–248. doi:10.1080/14786443309462277
- Montgomery, J. C., Jeffs, A., Simpson, S. D., Meekan, M. and Tindle, C.** (2006). Sound as an orientation cue for the pelagic larvae of reef fishes and decapod crustaceans. *Adv. Mar. Biol.* **51**, 143–196. doi:10.1016/S0065-2881(06)51003-X
- Myrberg, A. A. and Fuiman, L. A.** (2006). The sensory world of coral reef fishes. In *Coral Reef Fishes* (ed. P. F. Sale), pp. 123–148. New York: Academic Press.
- Nedelec, S. L., Campbell, J., Radford, A. N., Simpson, S. D. and Merchant, N. D.** (2016). Particle motion: the missing link in underwater acoustic ecology. *Methods Ecol. Evol.* **7**, 836–842. doi:10.1111/2041-210X.12544
- Parmentier, E., Mann, K. and Mann, D.** (2011). Hearing and morphological specializations of the mojarra (*Euclinostomus argenteus*). *J. Exp. Biol.* **214**, 2697–2701. doi:10.1242/jeb.058750
- Parmentier, E., Tock, J., Falguière, J.-C. and Beauchaud, M.** (2014). Sound production in *Sciaenops ocellatus*: preliminary study for the development of acoustic cues in aquaculture. *Aquaculture* **432**, 204–211. doi:10.1016/j.aquaculture.2014.05.017
- Parmentier, E., Berten, L., Rigo, P., Aubrun, F., Nedelec, S. L., Simpson, S. D. and Lecchini, D.** (2015). The influence of various reef sounds on coral-fish larvae behaviour. *J. Fish. Biol.* **86**, 1507–1518. doi:10.1111/jfb.12651
- Popper, A. N. and Fay, R. R.** (2011). Rethinking sound detection by fishes. *Hearing Res.* **273**, 25–36. doi:10.1016/j.heares.2009.12.023
- Popper, A. N. and Lu, Z.** (2000). Structure–function relationships in fish otolith organ. *Fish. Res.* **46**, 15–25. doi:10.1016/S0165-7836(00)00129-6
- Popper, A. N. and Schilt, C. R.** (2008). Hearing and acoustic behavior: basic and applied considerations. In *Fish Bioacoustics* (ed. J. F. Webb, R. R. Fay and A. N. Popper), pp. 17–48. New York: Springer Publishing.
- Radford, C. A., Stanley, J. A., Tindle, C. T., Montgomery, J. C. and Jeffs, A. G.** (2010). Localised coastal habitats have distinct underwater sound signatures. *Mar. Ecol. Prog. Ser.* **401**, 21–29. doi:10.3354/meps08451
- Radford, C. A., Montgomery, J. C., Caiger, P. and Higgs, D. M.** (2012). Pressure and particle motion detection thresholds in fish: a re-examination of salient auditory cues in teleosts. *J. Exp. Biol.* **215**, 3429–3435. doi:10.1242/jeb.073320
- Ramcharitar, J. and Popper, A. N.** (2004). Masked auditory thresholds in sciaenid fishes: a comparative study. *J. Acoust. Soc. Am.* **116**, 1687–1691. doi:10.1121/1.1771614
- Ramcharitar, J. U., Gannon, D. P. and Popper, A. N.** (2006a). Bioacoustics of fishes of the family Sciaenidae (Croakers and Drums). *T. Am. Fish. Soc.* **135**, 1409–1431. doi:10.1577/T05-207.1
- Ramcharitar, J. U., Higgs, D. M. and Popper, A. N.** (2006b). Audition in sciaenid fishes with different swim bladder-inner ear configurations. *J. Acoust. Soc. Am.* **119**, 439–443. doi:10.1121/1.2139068
- Rogers, P. H., Popper, A. N., Cox, M. and Saidel, W. M.** (1988). Processing of acoustic signals in the auditory system of bony fish. *J. Acoust. Soc. Am.* **83**, 338–349. doi:10.1121/1.396444
- Sand, O. and Hawkins, A. D.** (1973). Acoustic properties of the cod swimbladder. *J. Exp. Biol.* **58**, 797–820.
- Schilt, C. R., Cranford, T. W., Krysl, P., Shadwick, R. E. and Hawkins, A. D.** (2012). Vibration of the otoliths in a teleost. In *The Effects of Noise on Aquatic Life* (ed. A. N. Popper and A. Hawkins), pp. 105–107. New York: Springer Publishing.
- Schuijff, A. and Hawkins, A. D.** (1983). Acoustic distance discrimination by the cod. *Nature* **302**, 143–144. doi:10.1038/302143a0
- Schultz-Mirbach, T., Heß, M., Metscher, B. and Ladich, F.** (2012). Relationship between swim bladder morphology and hearing abilities—a case study on Asian and African cichlids. *PLoS ONE* **7**, e42292. doi:10.1371/journal.pone.0042292
- Schultz-Mirbach, T., Heß, M., Metscher, B. D. and Ladich, F.** (2013). A unique swim bladder-inner ear connection in a teleost fish revealed by a combined high-resolution microtomographic and three-dimensional histological study. *BMC Biol.* **11**, 75. doi:10.1186/1741-7007-11-75
- Simpson, S. D., Meekan, M., Montgomery, J., McCauley, R. and Jeffs, A.** (2005). Homeward sound. *Science* **308**, 221. doi:10.1126/science.1107406
- Simpson, S. D., Meekan, M. G., Jeffs, A., Montgomery, J. C. and McCauley, R. D.** (2008). Settlement-stage coral reef fish prefer the higher-frequency invertebrate-generated audible component of reef noise. *Anim. Behav.* **75**, 1861–1868. doi:10.1016/j.anbehav.2007.11.004
- Simpson, S. D., Meekan, M. G., Larsen, N. J., McCauley, R. D. and Jeffs, A.** (2010). Behavioral plasticity in larval reef fish: orientation is influenced by recent acoustic experiences. *Behav. Ecol.* **21**, 1098–1105. doi:10.1093/beheco/arq117
- Staaterman, E., Paris, C. B. and Helgers, J.** (2012). Orientation behavior in fish larvae: a missing piece to Hjort's critical period hypothesis. *J. Theor. Biol.* **304**, 188–196. doi:10.1016/j.jtbi.2012.03.016
- Staaterman, E., Paris, C. B. and Kough, A. S.** (2014). First evidence of fish larvae producing sounds. *Biol. Lett.* **10**, 20140643. doi:10.1098/rsbl.2014.0643
- Tavolga, W. N.** (1971). Sound production and detection. In *Fish Physiology*, Vol. 5 (ed. W. S. Hoar and D. J. Randall), pp. 135–205. New York: Academic Press.
- Tolimieri, N., Jeffs, A. and Montgomery, J. C.** (2000). Ambient sound as a cue for navigation by the pelagic larvae of reef fishes. *Mar. Ecol. Prog. Ser.* **207**, 219–224. doi:10.3354/meps207219
- Tolimieri, N., Haine, O., Jeffs, A., McCauley, R. and Montgomery, J.** (2004). Directional orientation of pomacentrid larvae to ambient reef sound. *Coral Reefs* **23**, 184–191. doi:10.1007/s00338-004-0383-0
- Tricas, T. C. and Boyle, K. S.** (2015). Sound pressure enhances the hearing sensitivity of *Chaetodon* butterflyfishes on noisy coral reefs. *J. Exp. Biol.* **218**, 1585–1595. doi:10.1242/jeb.114264

- Webb, J. F., Walsh, R. M., Casper, B. M., Mann, D. A., Kelly, N. and Cicchino, N.** (2012). Development of the ear, hearing capabilities and laterophysic connection in the spotfin butterflyfish (*Chaetodon ocellatus*). *Environ. Biol. Fish.* **95**, 275-290. doi:10.1007/s10641-012-9991-7
- Wright, K. J., Higgs, D. M., Belanger, A. J. and Leis, J. M.** (2005). Auditory and olfactory abilities of pre-settlement larvae and post-settlement juveniles of a coral reef damselfish (Pisces: Pomacentridae). *Mar. Biol.* **147**, 1425-1434. doi:10.1007/s00227-005-0028-z
- Wright, K. J., Higgs, D. M., Cato, D. H. and Leis, J. M.** (2010). Auditory sensitivity in settlement-stage larvae of coral reef fishes. *Coral Reefs* **29**, 235-243. doi:10.1007/s00338-009-0572-y
- Wright, K. J., Higgs, D. M. and Leis, J. M.** (2011). Ontogenetic and interspecific variation in hearing ability in marine fish larvae. *Mar. Ecol. Prog. Ser.* **424**, 1-13. doi:10.3354/meps09004
- Yan, H. Y., Fine, M. L., Horn, N. S. and Colón, W. E.** (2000). Variability in the role of the gasbladder in fish audition. *J. Comp. Physiol. A* **186**, 435-445. doi:10.1007/s003590050443